Research Article

Rockburst Prediction Based on the KPCA-APSO-SVM Model and Its Engineering Application

Yuefeng Li,[1] Chao Wang [ID],[1,2] Jiankun Xu,[3] Zonghong Zhou,[1,2] Jianhui Xu,[1] and Jianwei Cheng[3]

[1]*Faculty of Land Resource Engineering, Kunming University of Science and Technology, Yunnan, Kunming 650093, China*
[2]*Yunnan Key Laboratory of Sino-German Blue Mining and Utilization of Special Underground Space, Yunnan, Kunming 650093, China*
[3]*School of Safety Engineering, China University of Mining & Technology, Jiangsu, Xuzhou 221116, China*

Correspondence should be addressed to Chao Wang; wangchao@kust.edu.cn

The progress of construction and safe production in mining, water conservancy, tunnels, and other types of deep underground engineering is seriously affected by rockburst disasters. This makes it essential to accurately predict rockburst intensity. In this paper, the ratio of maximum tangential stress of surrounding rock to rock uniaxial compressive strength (σ_θ/σ_c), the ratio of rock uniaxial compressive strength to rock uniaxial tensile strength (σ_c/σ_t), and the elastic energy index of rock (W_{et}) were chosen as input indices, and rockbursts were graded as level I (none rockburst), level II (light rockburst), level III (medium rockburst), and level IV (strong rockburst). A total of 104 groups of rockburst engineering samples, collected widely from around the world, were divided into a training set (84 groups of samples) and a test set (20 groups of samples). Based on the kernel principal component analysis (KPCA), the adaptive particle swarm optimization (APSO) algorithm, and the support vector machine (SVM), the KPCA-APSO-SVM model was established. The proposed model showed satisfactory classification performance: the prediction accuracies of the training set and test set were 98.81% and 95%, respectively. In addition, the trained prediction model was applied to five rockburst engineering cases and compared with the BP neural network model, SVM model, and APSO-SVM model. The comparative results show that the KPCA-APSO-SVM model has a higher prediction accuracy; as such, it provides a new reliable method for rockburst prediction.

1. Introduction

As the depth of mining and tunneling increases, more and more underground projects are threatened by coal and gas outburst [1], rockburst [2], water inrush [3], and so forth. Rockburst is a kind of unexpected geological hazard caused by rock failure during excavation, accompanied by violent energy release [4, 5]. Along with the loosening, spalling, ejection, or even throwing of rocks, it often induces heavy casualties and great property loss [6–9]. In recent years, with the increase in geotechnical engineering with high buried depth, high in situ stress, and high geothermal temperature, rockbursts occur frequently, which has become a serious threat to engineering construction in many countries, such

as South Africa, Chile, China, Australia, Canada, Sweden, Norway, and others [10–14].

The accurate prediction of rockburst intensity is important for the prevention and control of rockbursts. To date, researchers have considered many single indices of rockburst prediction based on experimental or engineering experience, such as strength theory, stiffness theory, catastrophe theory, and similar. With the expanding of research, researchers have realized that single indices cannot effectively predict rockbursts under complex geological conditions. Owing to the numerous influencing factors involved in a rockburst, multiple indices are thought to be required simultaneously. At present, multi-index comprehensive prediction methods and machine learning methods have

often been used in rockburst prediction, including the support vector machine (SVM) method [15–17], random tree method [18], K-nearest neighbor method [19], Bayesian network method [20], extreme learning machine method [21], logical regression method [22], decision tree method [23], cloud model [24], artificial neural network [25], fuzzy comprehensive method [26], and expert method of hazard evaluation [27].

SVM is a classifier developed from the generalized portrait algorithm in pattern recognition. It is well-adapted for limited samples and widely used in classification and recognition. In the process of classification, SVM first maps low-dimensional data to high-dimensional space by kernel function to make the data as linearly separable as possible. There are numerous kernel functions, such as the linear kernel function (LKF), radial basis function (RBF), polynomial kernel function (PKF), and others. In the classification process of SVM, penalty factor c and kernel function parameter g are important parameters that affect classification performance. So far, researchers have developed many different SVM models to predict rockburst intensity. Yin et al. [7] established SVM models by ensemble learning layering technology and compared them with the SVM-RNN model and the KNN-SVM-DNN-RNN model. Zhou et al. [15] used the genetic algorithm (GA) and particle swarm optimization (PSO) algorithm to develop the GA-PSO-SVM model and compared it with the traditional SVM model. Pu et al. [16] applied the SVM model to predict the Kimberlite diamond mine's rockburst intensity and achieved strong results. Wu et al. [17] exploited the PSO algorithm to optimize the least squares support vector machine (LSSVM) and established a rockburst prediction model. Zhou et al. [19] used the supervised learning method to advance the SVM model and compared it with other models. Zhang et al. [28] introduced the beetle antennae search algorithm to optimize SVM and other machine learning methods. Much optimization work has been done on the SVM prediction model, but data preprocessing and model parameter adjustment still warrant further study.

The grid search method is carried out by conducting parameter optimization by traversing when the search range of the two parameters is determined. It depends on the setting of the search range and step. This is time-consuming and not conducive to building an efficient and accurate prediction model. Swarm intelligence algorithms can reduce the optimal time of parameters effectively and obtain the optimal parameters through information exchange in the group. PSO is an evolutionary computing method based on swarm intelligence that uses cooperation and information sharing among individuals in the group to find the best optimal solution. However, it has weaknesses in its application, such as precocity convergence and poor ability for local optimization. Thus, an adaptive particle swarm optimization (APSO) algorithm is proposed to optimize the two important parameters c and g in the paper. Further, the kernel principal component analysis (KPCA) method and the improved SVM are used to process the rockburst prediction indices and train the samples, respectively, and the novel KPCA-APSO-SVM model is established to predict rockburst risk.

2. Principle of the Method

2.1. The KPCA Method.
KPCA is a nonlinear principal component analysis method based on the kernel method. The kernel method is a learning algorithm based on kernel function that mainly solves nonlinear pattern analysis problems. Figure 1 shows the core idea of the kernel method; that is, to define a nonlinear function Φ, map the original space to a higher-dimensional space and then carry out the linear operation in the higher-dimensional space to complete the nonlinear operation of the original space.

The kernel method can avoid the explicit expression of nonlinear mapping and reduce computational complexity. The principle of the kernel function can be described by the following equation:

$$\left(x_i, x_j\right) \Longrightarrow K\left(x_i, x_j\right) = \langle \Phi\left(x_i\right) \bullet \Phi\left(x_j\right) \rangle, \tag{1}$$

where $\left(x_i, x_j\right)$ is the inner product of the original space, Φ is the nonlinear function mapped to the high-dimensional space, and the kernel function transforms the inner product of the high-dimensional space into the function calculation of the original space x and does not need to explicitly give the expression of Φ. The commonly used five types of kernel functions are presented in Table 1.

2.2. SVM

2.2.1. The Principle of SVM.
SVM, a supervised learning algorithm, is used for data analysis and classification decisions based on statistical learning theory and the principle of structural risk minimization. It uses limited sample information to establish the classification hyperplane in the feature space and gains the abilities of classification and recognition with the advantages of fewer sample requirements, nonlinear and high dimensional space. In the classification process, SVM maps low-dimensional data to high-dimensional space with the help of kernel function. Due to the RBF kernel function can achieve good classification performance in large or small samples and high-dimensional or low-dimensional data [29], we choose RBF kernel function to map low-dimensional data to high-dimensional space.

2.2.2. The Calculation Process of SVM.
The data set $D = [(x_1, y_1), \ldots, (x_l, y_l)]$ is sampled and set in the n-dimensional space, and the decision function is $f(x) = \omega \cdot k(x) + b$, where ω, b, and $k(x)$ are the weight vector, domain value, and nonlinear mapping function, respectively [30]. The optimization of the classification plane constraint should meet the following condition:

$$y_i\left(\omega^T \cdot k\left(x_i\right) + b\right) \geq 1. \tag{2}$$

Nonnegative relaxation variables $\xi_i s$ are introduced to convert the optimization problem into the following equation:
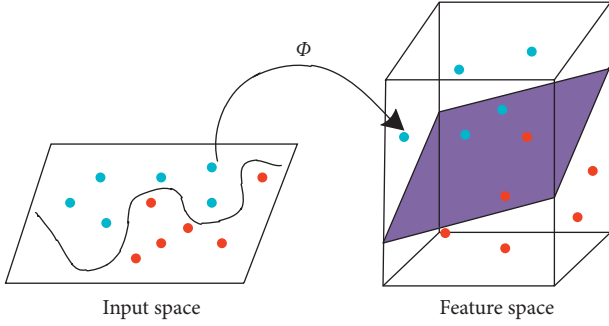
FIGURE 1: The core idea of the kernel method.

TABLE 1: Commonly used kernel functions.

Kernel function type	Kernel function expression
Linear kernel function (LKF)	$K(x_i, x_j) = x_i^T \bullet x_j + c$
Polynomial kernel function (PKF)	$K(x_i, x_j) = (ax_i^T x_j + c)^q$
Radial basis function (RBF)	$K(x_i, x_j) = \exp(-g\|x_i - x_j\|^2)$
Sigmoid kernel function (SKF)	$K(x_i, x_j) = \tanh(v(x_i \bullet x_j) + c)$
Gaussian kernel function (GKF)	$K(x_i, x_j) = \exp(-(\|x_i - x_j\|^2 / 2\sigma^2))$

Note. c, a, v, and g are manually set parameters, q is the degree of a polynomial, and σ is the gauss kernel bandwidth.

$$\begin{cases} \min & \dfrac{1}{2}\|\omega\|^2 + c\sum_{i=1}^{n}\xi_i \\ \\ \text{s.t.} & y_i(\omega^T \cdot k(x_i) + b) \geq 1 - \xi_i, \end{cases} \tag{3}$$

where c is a penalty parameter $(c > 0)$ that represents a punishment for misclassification, used to reconcile the coefficient with the maximum interval and the minimum number of misclassification points. The penalty value for misclassification increases with the addition of c. Here, the Lagrange multiplier algorithm is introduced to obtain the following equation:

$$L(\omega, b, a_i) = \frac{1}{2}\|\omega\|^2 + \sum_{i=1}^{n} a_i(1 - y_i(\omega^T \cdot k(x_i) + b)), \quad a_i = (a_1, a_2, \ldots, a_n). \tag{4}$$

The partial derivatives of ω and b in Lagrange function $L(\omega, b, a_i)$ are obtained as per the following equation:

$$\begin{cases} \omega = \sum_{i=1}^{m} a_i y_i x_i, \\ \\ b = \sum_{i=1}^{m} a_i y_i. \end{cases} \tag{5}$$

The Lagrange multiplier algorithm is introduced to obtain the following equation:

$$L(\omega, b, a_i) = \sum_{i=1}^{n} a_i - \frac{1}{2}\sum_{i=1}^{n}\sum_{j=1}^{n} a_i a_j y_i y_j x_i^T x_j, \tag{6}$$

namely, $\min_{\omega, b} L(\omega, b, a) = \sum_{i=1}^{n} a_i - (1/2)\sum_{i=1}^{n}\sum_{j=1}^{n} a_i a_j y_i y_j x_i x_j$. Then, the optimization problem is transformed into a duality problem:

$$\begin{cases} \min & \dfrac{1}{2}\sum_{i=1}^{n}\sum_{j=1}^{n} y_i y_j a_i a_j K(x_i, x_j) - \sum_{i=1}^{n} a_i \\ \\ \text{s.t.} & \sum_{i=1}^{n} y_i a_i = 0, 0 \leq a_i \leq c, \end{cases} \tag{7}$$

where the RBF kernel function $K(x_i, x_j) = (k(x_i) \cdot k(x_j))$ adopted in this paper is as follows:

$$K(x_i, x_j) = \exp\left(-g\|x_i - x_j\|\right)^2, \tag{8}$$

where g is the kernel function parameter; the above optimization problem can be converted to

$$\begin{cases} \min & \dfrac{1}{2}\sum_{i=1}^{n}\sum_{j=1}^{n} y_i y_j a_i a_j \exp\left(-g\|x_i - x_j\|\right)^2 - \sum_{i=1}^{n} a_i \\ \\ \text{s.t.} & \sum_{i=1}^{n} y_i a_i = 0, 0 \leq a_i \leq c. \end{cases} \tag{9}$$

2.2.3. Process Derivation of the PSO Algorithm. According to equation (9), c and g affect the classification performance of SVM. Then, the PSO algorithm is introduced for parameter optimization with the classical iterative formulas as follows:

$$\begin{cases} v(t+1) = \overline{\omega}t + c_1 r_1 (q_{\text{best}}(t) - q(t)) + c_2 r_2 (p_{\text{best}}(t) - q(t)), \\ q(t+1) = q(t) + v(t+1), \end{cases} \tag{10}$$

where $v(t)$ is the velocity of particles at time t; $\overline{\omega}$ is the inertia weight; $q_{\text{best}}(t)$, $q(t)$, and $p_{\text{best}}(t)$ represent the optimal solution, solution, and global optimal solution of particles at time t, respectively; r_1 and r_2 are random numbers belonging to the range [0,1]; and c_1 and c_2 are learning factors.

In the classical PSO algorithm, $\overline{\omega}$ describes the influence of the previous generation of particles on the current generation. The larger the search ranges of particles, the stronger the global optimization ability and the ability to avoid falling

into the local optimal solution. The PSO algorithm adjusts the balance between global search and local optimal capabilities. The calculation equation of $\overline{\omega}$ is described as follows:

$$\overline{\omega} = \overline{\omega}_{\text{max}} - \frac{\overline{\omega}_{\text{max}} - \overline{\omega}_{\text{min}}}{N_{\text{max}}} \cdot N, \qquad (11)$$

where $\overline{\omega}_{\text{max}} = 0.9$ is the maximum inertia weight, $\overline{\omega}_{\text{min}} = 0.3$ is the minimum inertia weight, N_{max} is the maximum iteration algebra, and N is the current iteration algebra.

Equation (11) shows that value $\overline{\omega}$ is at the maximum at the beginning of the iteration, and the particle has a wide range when conducting a global search. With the increase in iteration times, the particle gradually approaches the global optimal solution. Meanwhile, the value of $\overline{\omega}$ decreases, and the particle can search locally in a small range and ultimately obtain the global optimal solution. The $\overline{\omega}$ value varies with the number of iterations, and so it is called the adaptive inertia weight.

c_1 and c_2 reflect the information exchange between single particles and the information exchange between the total number of particles and the historical optimal trajectory, respectively. Asynchronous learning can effectively exchange information between particles [31]. This paper adjusts the two parameters through an asynchronous learning formula, and the adjusted equation is as follows:

$$\begin{cases} c_1 = 2 - \dfrac{1}{N_{\text{max}}} \cdot N, \\[2mm] c_2 = 1 + \dfrac{1}{N_{\text{max}}} \cdot N. \end{cases} \qquad (12)$$

To effectively control the flying speed of particles and allow the algorithm to achieve an effective balance between global detection and local excavating, the compression coefficient β is introduced as follows:

$$\beta = \frac{2}{\left| 2 - c - \sqrt{c^2 - 4c} \right|}, \qquad (13)$$

where $c = c_1 + c_2$.

Finally, we propose an APSO algorithm with a compression factor and an asynchronous learning factor, as shown in the following equation:

$$\begin{cases} v(t+1) = \beta \left(\overline{\omega} t + c_1 r_1 \left(q_{\text{best}}(t) - q(t) \right) + c_2 r_2 \left(p_{\text{best}}(t) - q(t) \right) \right), \\[2mm] q(t+1) = q(t) + v(t+1). \end{cases} \qquad (14)$$

3. Dataset Preparations

To date, many indices have been used in rockburst prediction. Comprehensively considering internal factors (such as the physical and mechanical properties of rock), external factors (e.g., stress concentration caused by excavation) for rockburst, and index selection requirements (e.g., scientificity, practicability, and quantifiable), σ_θ/σ_c, σ_c/σ_t, and W_{et} were selected as input indices. The rockbursts were graded into four levels: level I (none), level II (light), level III (medium), and level IV (strong).

104 groups of well-documented rockburst samples, including 20 groups of level I samples, 28 groups of level II samples, 37 groups of level III samples, and 19 groups of level IV samples, were collected by consulting the literature. Part of the rockburst samples is presented in Table 2. Figure 2 is a box chart of three input indices that shows the median line, mean value, maximum value, minimum value, and 25~75% of the index range and outliers, where Figures 2(a)–2(c) are a boxplot of σ_θ/σ_c, σ_c/σ_t, and W_{et}, respectively; and Figure 2(d) is the overall boxplot of three input indices. As seen in Figure 2, there are a small number of outliers in each group of data, and the data distribution is asymmetric, especially in Figure 2(c). In order to ensure the objectivity of the sample data, this paper does not replace the outliers.

4. Methods

104 groups of rockburst samples were divided into a training set and a test set. The training set was composed of 15 groups of level I samples, 23 groups of level II samples, 32 groups of level III samples, and 14 groups of level IV samples selected randomly in this paper, and the test set was made up of the remaining 20 groups of samples. Fivefold cross-validation was performed on the training set, as shown in Figure 3. Its basic idea is to divide all samples into five parts, take one part as the test set each time without repetition, take the other four parts as the training set to train the model, then to calculate the error rate Ei ($i = 1, 2, 3, 4, 5$) of the model used in the test set, and finally to calculate the average value of Ei to get the comprehensive error rate E. And classification accuracy, $F1$-score value, and Kappa coefficient were used to evaluate the performance of the prediction model. The construction process of the KPCA-APSO-SVM model is presented in Figure 4.

5. Experiment and Analysis

5.1. Data Process and Analysis in KPCA. Data processing directly affects classification performance. This necessitates the preprocessing of the characteristic data that affect the rockburst prediction result. In order to ensure that the information of each variable does not interfere with others and to mine the rich data association between features from high-dimensional space, this paper uses KPCA to process the data, selects the best KPCA dimension reduction effect through the comparison of different kernel parameters, and uses the principal component analysis (PCA) method to process the data. It compares the results to KPCA.

TABLE 2: Part of the rockburst samples.

No.	Prediction indices			Actual level
	σ_θ/σ_c	σ_c/σ_t	W_{et}	
1	0.11	31.2	7.4	I
2	0.10	23.0	5.7	I
3	0.20	36.0	2.3	I
4	0.44	13.1	2.1	II
5	0.37	24.0	5.1	II
. . .	. . .	. . .	. . .	. . .
100	0.66	22.3	3.2	III
101	0.72	27.5	4.3	III
102	0.62	19.4	4.5	III
103	0.64	17.5	7.2	IV
104	0.65	12.4	5.4	IV

(a)

(b)

(c)

(d)
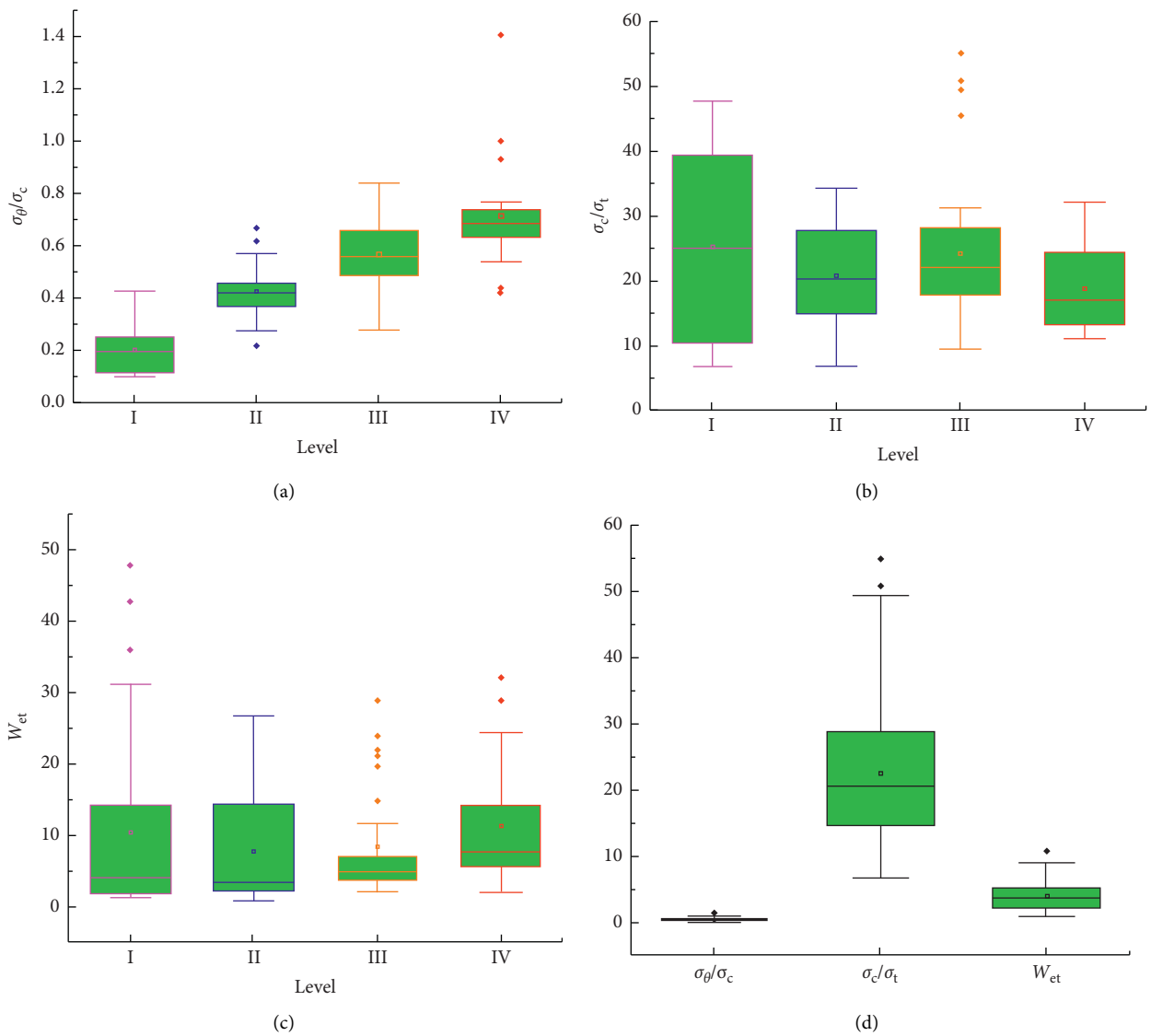
FIGURE 2: Box chart of input indices: (a) σ_θ/σ_c; (b) σ_c/σ_t; (c) W_{et}; (d) three indices.

PCA is an unsupervised data processing method that renders the feature-transformed principal parts independent of each other through linear transformation.

Figure 5 is the dimension reduction map obtained by the traditional PCA dimensionality reduction method. The clustering effect of each rockburst grade sample point in
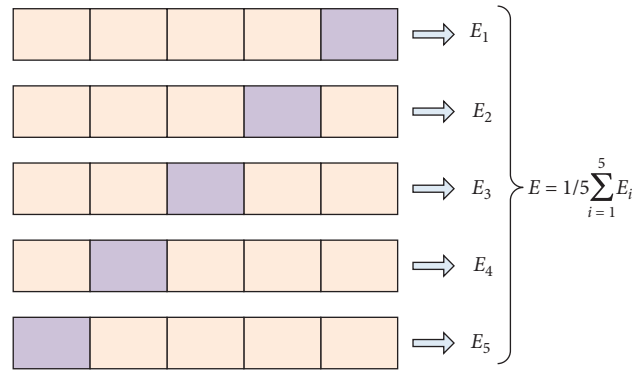
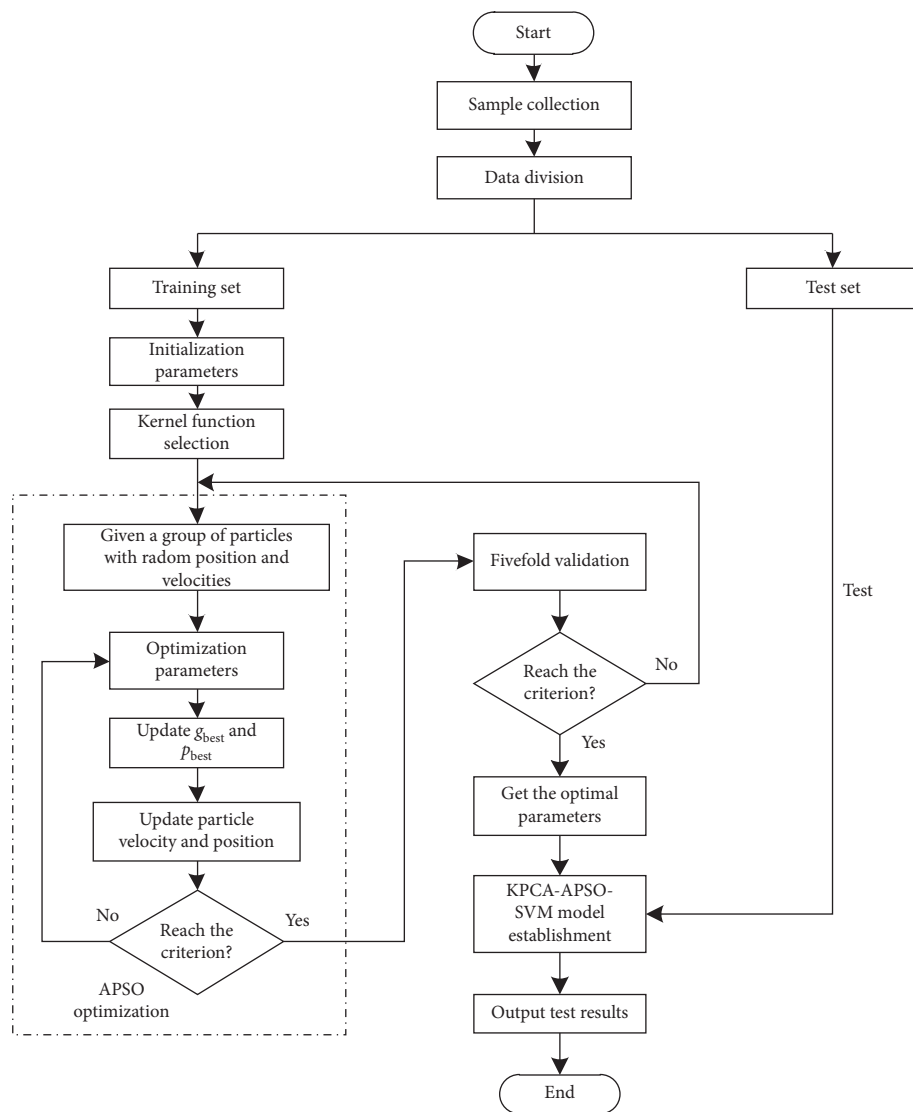FIGURE 3: Fivefold cross-validation.

FIGURE 4: Construction flow of the KPCA-APSO-SVM model.

the two-dimensional dimension reduction map obtained by the first and second dimensionality reduction principal components PC1 and PC2 is not evident. There are too many overlapping samples, and the information difference between the various samples is very inconspicuous, which indicates that the relationship between the original

feature data cannot make the PCA processed data have a clearer clustering effect.

KPCA is a supervised data processing method. Its primary task is to determine the kernel function, but there is no clear guiding principle at present. The RBF kernel function is often the first choice for the KPCA kernel function because it has a small deviation in the case of less-relevant conditions. Therefore, the RBF kernel function is selected in this paper. First, KPCA is used to map the low-dimensional data to the high-dimensional space so that the features between the data are linearized, and then the linear transformation of PCA is used to achieve the purpose of data dimension reduction. Differing from traditional KPCA, the main method of data processing based on dimension reduction, the KPCA method adopted in this paper mainly mines the association between features in high-dimensional space through dimension elevation, which makes the processed data easier to classify.

Figure 6 is the two-dimensional dimensionality reduction graph after data processing of the original features with different values of kernel function parameter C. The value of C affects the data processing effect of KPCA. Different values of C ($C = 10$, 20, 50, 100) were selected to undertake a comparative study. When the C value is greater than 100, the data processing effect remains unchanged. It can be seen from Figure 6 that when $C = 10$, the processing effect is evidently better than the PCA clustering effect, and the effect becomes gradually obvious with the increase in kernel function parameters. When $C = 100$, compared with the traditional PCA dimensionality reduction and other kernel function parameters, the processing effect is the most obvious. After calculation, this paper selects 8 kernel principal components, KPC1~KPC8, whose cumulative contribution rate is greater than 90%, for data analysis. The kernel principal components of some samples are shown in Table 3, and the cumulative contribution rate is presented in Table 4.

5.2. Processing and Analysis of SVM.
The penalty parameter c and kernel function parameter g are important parameters that affect SVM classification performance. In this paper, an APSO algorithm is proposed to optimize c and g. The PSO's fitness function is the maximum accuracy of the fivefold cross-validation of the training set. The optimal parameters c and g are obtained when reaching the maximum accuracy value. During the initialization process of APSO, the numbers of particles with the same speed and iterations are 30 and 50, respectively.

The optimization process of SVM parameters both without and after KPCA processing is presented in Figure 7. In the parameter optimization curve without KPCA processing, when the fivefold cross-validation accuracy of the training set reaches 91.67%, the optimal value of c is 100 and that of g is 0.01. In the parameter optimization curve after KPCA processing, when the fivefold cross-validation accuracy of the training set reaches 98.81%, the optimal value of c is 78.4885 and that of g is 0.62947.

After obtaining the optimal parameters, the APSO-SVM classification model was established. Figure 8 shows the classification results without as well as after KPCA
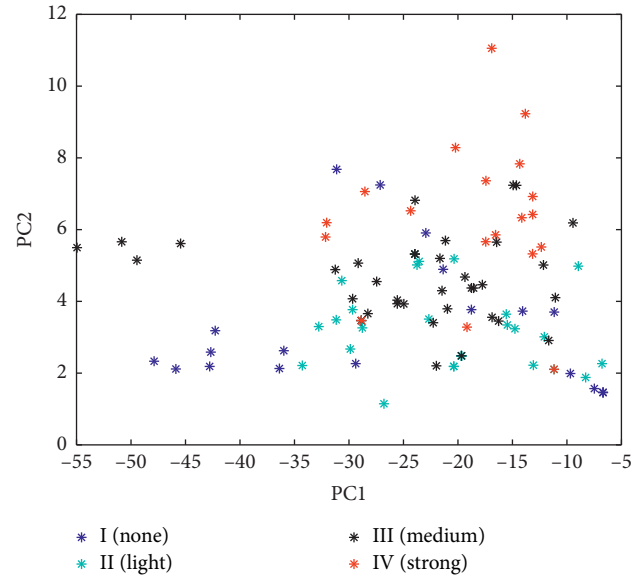

FIGURE 5: PCA dimension reduction data.

processing. The Arabic numerals 1, 2, 3, and 4 on the ordinate of the figure indicate rockburst risk level I, level II, level III, and level IV, respectively. It can be seen that the former contains four misjudgments, while the latter contains only one misjudgment. The classification accuracy is higher after KPCA processing.

5.3. Performance Evaluation.
Three parameters, namely, classification accuracy, the F1-score value, and the Kappa coefficient were used to evaluate the model classification performance. When the F1-score value was close to 1, this indicated that the classifier has strong comprehensive classification ability. When the Kappa coefficient was close to 1, this indicated that the actual output is consistent with the predicted output. Table 5 shows the evaluation results of the APSO-SVM model and the KPCA-APSO-SVM model, in which the optimal classification accuracies of the training set, test set, F1-score, and Kappa coefficient were 98.81%, 95%, 0.9495, and 0.9333 respectively, all from the KPCA-APSO-SVM model. We can see that the classification performance of the model treated by KPCA is significantly better than that of the model not treated by KPCA and that the classification accuracy of the model is greatly improved after KPCA processing for rockburst samples.

6. Engineering Verification

We applied the KPCA-APSO-SVM model to predict the rockburst intensity of five engineering cases, which included the Jinping II hydropower station diversion tunnel (case 1), the copper mine of Huaxi Group Co. Ltd. (case 2), the Jinchuan No. 2 mine (case 3), the Daxiangling tunnel (case 4), and the Dongguashan copper mine (case 5). Then, based on the same training sample set, we established the BP neural network (BPNN) model and the SVM model, respectively, to carry out a comparative study of the prediction results.
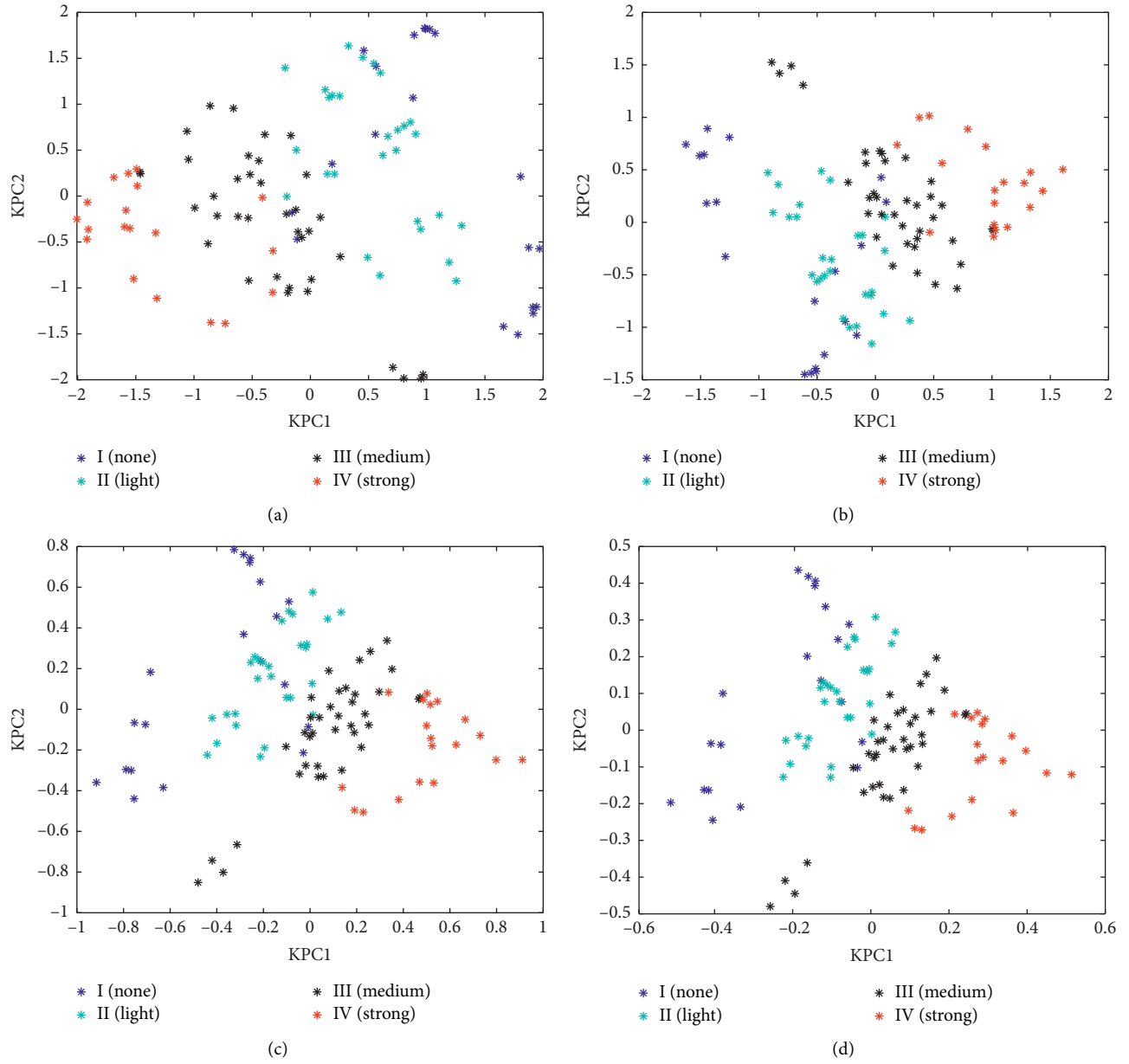
(a)

(b)

(c)

(d)

Figure 6: KPCA dimension reduction results: (a) $C = 10$; (b) $C = 20$; (c) $C = 50$; (d) $C = 100$.

Table 3: Kernel principal components of some samples.

No.	KPC1	KPC2	KPC3	KPC4	KPC5	KPC6	KPC7	KPC8
1	0.10692	0.42853	1.97035	−0.17271	0.65215	−0.22392	0.10120	0.24332
2	−0.25321	−0.38902	1.85827	0.20085	0.53811	−0.26607	0.06083	−0.03937
3	−1.95496	0.79475	0.77955	0.01823	−0.29556	−0.32993	−0.04782	−0.16777
4	−1.84689	1.49646	0.87969	−0.60029	−0.48013	−0.27125	0.19077	−0.16795
5	−1.30235	−1.72574	0.42354	−0.82812	0.05384	0.41649	−0.31473	−0.12872
. . .	. . .	. . .	. . .	. . .	. . .	. . .	. . .	. . .
100	1.77102	0.05669	−0.30371	−0.06907	−0.23411	0.00553	0.03396	−0.16156
101	1.52412	1.06352	0.41351	−0.01057	0.01023	0.30916	−0.25692	−0.01365
102	1.68988	0.20107	1.51051	−0.26358	−0.02316	−0.12874	−0.15304	0.29054
103	2.08223	0.23528	0.58012	−0.27131	−0.32644	−0.00912	−0.14021	−0.01348
104	1.61922	−0.41878	−0.28636	−0.11999	−0.29266	−0.03638	0.19072	−0.13508

TABLE 4: Cumulative contribution rate of KPC.

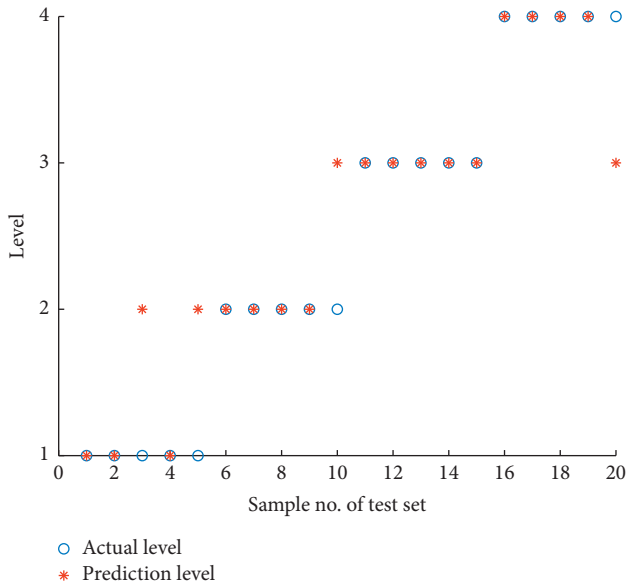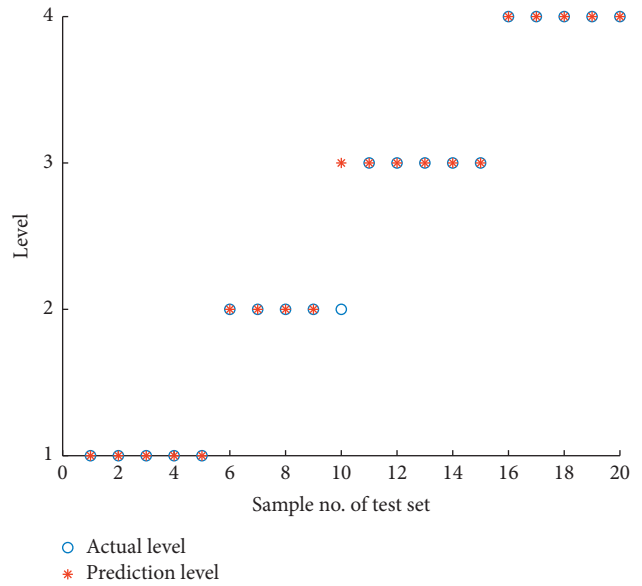| Core principal component	Cumulative contribution rate (%)
KPC1	23.91
KPC2	45.99
KPC3	65.92
KPC4	75.99
KPC5	81.08
KPC6	85.86
KPC7	89.12
KPC8	92.01
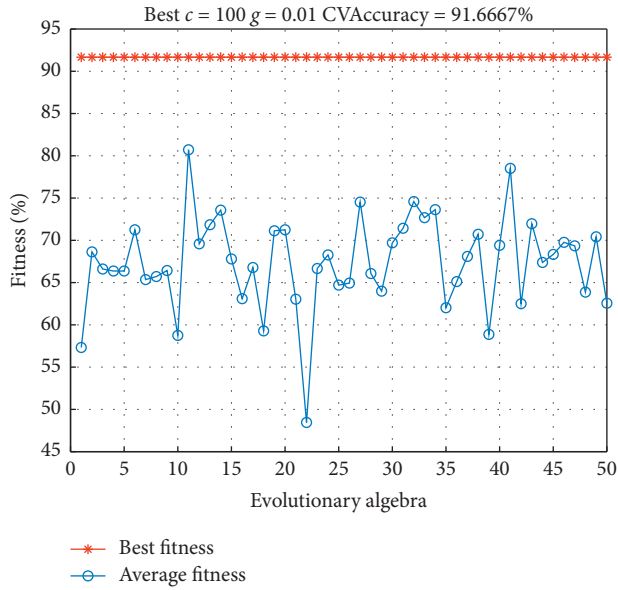
(a)
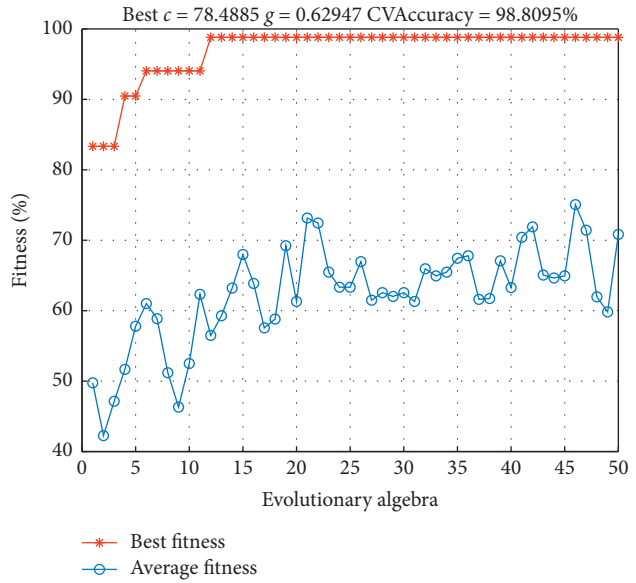
(b)

FIGURE 7: Optimization process of SVM model parameters: (a) without KPCA processing; (b) after KPCA processing.

(a)

(b)

FIGURE 8: Classification results: (a) without KPCA processing; (b) after KPCA processing.

TABLE 5: Classification performance comparison.

Model	Training set accuracy (%)	Test set accuracy (%)	F1-score	Kappa coefficient
APSO-SVM	91.67	80	0.7999	0.7333
KPCA-APSO-SVM	98.81	95	0.9495	0.9333

TABLE 6: Prediction results of engineering cases.

No.	Reference	Prediction indices			Actual level	Prediction results			
		σ_θ/σ_c	σ_c/σ_t	W_{et}		BPNN	SVM	APSO-SVM	KPCA-APSO-SVM
1	[15]	0.62	20.0	3.1	III	III	III	III	III
2	[32]	0.61	17.9	5.3	III	III	III	III	III
3	[33]	0.44	13.1	2.1	II	II	I	II	II
4	[34]	0.71	32.2	5.5	IV	III	III	IV	IV
5	[35]	0.47	11.0	4.0	III	II	III	III	III

The prediction results of the four models are presented in Table 6. As we can see from the table, the BPNN model misjudged the rockburst grade of case 4 from level IV to III and of case 5 from level III to II. The SVM model misjudged the rockburst grade of case 3 from level II to I and of case 4 from level IV to III. The prediction results of the APSO-SVM model and the KPCA-APSO-SVM model were all accurate and completely consistent with the situation in the field. Thus, compared with the traditional SVM model and the BPNN model, the prediction effect of the SVM model optimized by APSO is better. This shows that APSO has a good optimization effect. Although the APSO-SVM model and the KPCA-APSO-SVM model have the same prediction results, Table 5 shows that the classification accuracy, F1-score, and Kappa coefficient of the KPCA-APSO-SVM model are all greater than those of the APSO-SVM model. Therefore, the KPCA-APSO-SVM model has higher application value under the same conditions.

Compared with the traditional SVM model and other models, the KPCA-APSO-SVM model can better optimize the parameters c and g, which affect the classification performance of SVM and thus obtain a higher prediction accuracy for rockbursts.

7. Conclusion

(1) In this paper, σ_θ/σ_c, σ_c/σ_t, and W_{et} were selected as input indices of SVM, and 104 groups of rockburst engineering samples were divided into a training set (84 groups of samples) and a test set (20 groups of samples). The APSO algorithm was proposed to optimize the penalty parameter c and kernel function parameter g of SVM, which improved the classification performance of SVM.

(2) KPCA, under different kernel parameters C ($C = 10$, 20, 50, 100), was used to process the rockburst sample data. The results show that the processing effect of KPCA was best when $C = 100$. Eight principal components with cumulative variance contribution rates over 90% were extracted, and the APSO-SVM model and KPCA-APSO-SVM model were established combined with the APSO algorithm. The comparison results show that the

KPCA-APSO-SVM model has a higher prediction accuracy, F1-score, and Kappa coefficient, and so the prediction effect of the model built by using the sample data processed by KPCA is better.

(3) The novel KPCA-APSO-SVM model was validated by five engineering cases, and the prediction results were completely consistent with the practical rockburst situations. They were better than the BPNN model and the traditional SVM model, indicating that the proposed model was an efficient and practical rockburst intensity classification prediction model.

Data Availability

The data used to support the findings of this study are available from the corresponding author upon request.

Conflicts of Interest

The authors declare that they have no conflicts of interest.

Acknowledgments

References

[1] X. Wu, Y. Peng, J. Xu, Q. Yan, W. Nie, and T. Zhang, "Experimental study on evolution law for particle breakage during coal and gas outburst," *International Journal of Coal Science & Technology*, vol. 7, no. 1, pp. 97–106, 2020.

[2] A. I. Kopytov, A. A. Eremenko, and Y. N. Shaposhnik, "Design of support systems for rockburst-hazardous underground minesin Gornaya Shoria," *Journal of Mining Science*, vol. 56, no. 4, pp. 567–574, 2020.

[3] E. Hou, Q. Wen, Z. Ye, W. Chen, and J. Wei, "Height prediction of water-flowing fracture zone with a genetic-

algorithm support-vector-machine method," *International Journal of Coal Science & Technology*, vol. 7, no. 4, pp. 740–751, 2020.

[4] K. G. Li, M. L. Li, and Q. C. Qin, "Research on evaluation method of rock burst tendency based on improved comprehensive weighting," *Chinese Journal of Rock Mechanics and Engineering*, vol. 39, no. S1, pp. 2751–2762, 2020.

[5] D. Song, E. Wang, H. He et al., "Use of electromagnetic radiation from fractures for mining-induced stress field assessment," *Journal of Geophysics and Engineering*, vol. 15, no. 4, pp. 1093–1103, 2018.

[6] F. Q. Gong, Y. L. Wang, Z. G. Wang, J. F. Pan, and S. Luo, "A new criterion of coal burst proneness based on the residual elastic energy index," *International Journal of Mining Science and Technology*, vol. 11, 2021.

[7] X. Yin, Q. Liu, Y. Pan, X. Huang, J. Wu, and X. Wang, "Strength of stacking technique of ensemble learning in rockburst prediction with imbalanced data: comparison of eight single and ensemble models," *Natural Resources Research*, vol. 30, no. 2, pp. 1795–1815, 2021.

[8] W. Pytel, J. Świtoń, and A. Wójcik, "The effect of mining face's direction on the observed seismic activity," *International Journal of Coal Science & Technology*, vol. 3, no. 3, pp. 322–329, 2016.

[9] S. He, D. Song, Z. Li et al., "Precursor of spatio-temporal evolution law of MS and AE activities for rock burst warning in steeply inclined and extremely thick coal seams under caving mining conditions," *Rock Mechanics and Rock Engineering*, vol. 52, no. 7, pp. 2415–2435, 2019.

[10] R. Altindag, "Correlation of specific energy with rock brittleness concepts on rock cutting," *Journal of the South African Institute of Mining and Metallurgy*, vol. 103, no. 3, pp. 163–171, 2003.

[11] R. K. Wattimena, B. Sirait, N. P. Widodo, and K. Matsui, "Evaluation of rockburst potential in a cut-and-fill mine using energy balance," *International Journal of the JCRM*, vol. 8, no. 1, pp. 19–23, 2012.

[12] F.-Q. Gong, C. Wu, S. Luo, and J.-Y. Yan, "Load-unload response ratio characteristics of rock materials and their application in prediction of rockburst proneness," *Bulletin of Engineering Geology and the Environment*, vol. 78, no. 7, pp. 5445–5466, 2019.

[13] Y. L. Chen, J. P. Zuo, D. J. Liu, Y. J. Li, and Z. B. Wang, "Experimental and numerical study of coal-rock bimaterial composite bodies under triaxial compression," *International Journal of Coal Science & Technology*, vol. 8, p. 12, 2021.

[14] X. Xi, X. Wu, Q. Guo, and M. Cai, "Experimental investigation and numerical simulation on the crack initiation and propagation of rock with pre-existing cracks," *IEEE Access*, vol. 8, Article ID 129636, 2020.

[15] J. Zhou, X. Li, and X. Shi, "Long-term prediction model of rockburst in underground openings using heuristic algorithms and support vector machines," *Safety Science*, vol. 50, no. 4, pp. 629–644, 2012.

[16] Y. Pu, D. B. Apel, and H. Xu, "Rockburst prediction in kimberlite with unsupervised learning method and support vector classifier," *Tunnelling and Underground Space Technology*, vol. 90, pp. 12–18, 2019.

[17] S. C. Wu, Z. G. Wu, and C. X. Zhang, "Rock burst prediction probability model based on case analysis," *Tunnelling and Underground Space Technology*, vol. 93, p. 15, Article ID 103069, 2019.

[18] M. Ahmad, J. L. Hu, M. Hadzima-Nyarko et al., "Rockburst hazard prediction in underground projects using two intelligent classification techniques: a comparative study," *Symmetry-Basel*, vol. 13, no. 4, p. 18, 2021.

[19] J. Zhou, X. B. Li, and H. S. Mitri, "Classification of rockburst in underground projects: comparison of ten supervised learning methods," *Journal of Computing in Civil Engineering*, vol. 30, no. 5, Article ID 04016003, 2016.

[20] N. Li, R. Jimenez, and X. Feng, "The influence of Bayesian networks structure on rock burst hazard prediction with incomplete data," *Procedia Engineering*, vol. 191, pp. 206–214, 2017.

[21] T.-Z. Li, Y.-X. Li, and X.-L. Yang, "Rock burst prediction based on genetic algorithms and extreme learning machine," *Journal of Central South University*, vol. 24, no. 9, pp. 2105–2113, 2017.

[22] N. Li and R. Jimenez, "A logistic regression classifier for long-term probabilistic prediction of rock burst hazard," *Natural Hazards*, vol. 90, no. 1, pp. 197–215, 2017.

[23] E. Ghasemi, H. Gholizadeh, and A. C. Adoko, "Evaluation of rockburst occurrence and intensity in underground structures using decision tree approach," *Engineering with Computers*, vol. 36, no. 1, pp. 213–225, 2020.

[24] Y. Lin, K. Zhou, and J. Li, "Application of cloud model in rock burst prediction and performance comparison with three machine learning algorithms," *IEEE Access*, vol. 6, Article ID 30958, 2018.

[25] L. Ribeiro e Sousa, T. Miranda, R. Leal e Sousa, and J. Tinoco, "The use of data mining techniques in rockburst risk assessment," *Engineering*, vol. 3, no. 4, pp. 552–558, 2017.

[26] A. C. Adoko, C. Gokceoglu, L. Wu, and Q. J. Zuo, "Knowledge-based and data-driven fuzzy modeling for rockburst prediction," *International Journal of Rock Mechanics and Mining Sciences*, vol. 61, pp. 86–95, 2013.

[27] J. Kornowski and J. Kurzeja, "Prediction of rockburst probability given seismic energy and factors defined by the expert method of hazard evaluation (MRG)," *Acta Geophysica*, vol. 60, no. 2, pp. 472–486, 2012.

[28] J. F. Zhang, Y. H. Wang, Y. T. Sun, and G. C. Li, "Strength of ensemble learning in multiclass classification of rockburst intensity," *International Journal for Numerical and Analytical Methods in Geomechanics*, vol. 44, no. 13, 2020.

[29] Y. Li, J. Zhang, T. Li, H. Liu, J. Li, and Y. Wang, "Geographical traceability of wild Boletus edulis based on data fusion of FT-MIR and ICP-AES coupled with data mining methods (SVM)," *Spectrochimica Acta Part A: Molecular and Biomolecular Spectroscopy*, vol. 177, pp. 20–27, 2017.

[30] Y. Shi, F. Gong, M. Wang, J. Liu, Y. Wu, and H. Men, "A deep feature mining method of electronic nose sensor data for identifying beer olfactory information," *Journal of Food Engineering*, vol. 263, pp. 437–445, 2019.

[31] Y. Zhao and Z. Fang, "Particle swarm optimization algorithm with weight function's learning factor," *Journal of Computer Applications*, vol. 33, no. 8, pp. 2265–2268, 2013.

[32] K. P. Zhou, T. Lei, and J. H. Hu, "RS-TOPSIS model of rockburst prediction in deep metal mines and its application," *Chinese Journal of Rock Mechanics and Engineering*, vol. 32, no. S2, pp. 3705–3711, 2013.

[33] Y. L. Yi, P. Cao, and C. Z. Pu, "Multi-factorial comprehensive estimation for Jinchuan's deep typical rockburst tendency," *Science and Technology Review*, vol. 28, no. 2, pp. 76–80, 2010.

[34] J. F. Zhang, *Study on Prediction by Stages and Control Technology of Rockburst Hazard of Daxiangling Hinghway Tunnel*, Southwest Jiaotong University, Chengdu, China, 2010.

[35] Z. J. Liu, Q. P. Yuan, and J. L. Li, "Application of fuzzy probability model to prediction of classification of rockburst intensity," *Chinese Journal of Rock Mechanics and Engineering*, vol. 27, no. S1, pp. 3095–3103, 2008.